

Magnetization dynamics and Gilbert damping in ultrathin $\text{Co}_{48}\text{Fe}_{32}\text{B}_{20}$ films with out-of-plane anisotropy

G. Malinowski,^{a)} K. C. Kuiper, R. Lavrijsen, H. J. M. Swagten, and B. Koopmans
 Department of Applied Physics, Center for NanoMaterials, Eindhoven University of Technology,
 P.O. Box 513, 5600 MB Eindhoven, The Netherlands

(Received 1 December 2008; accepted 11 February 2009; published online 9 March 2009)

Time resolved magneto-optical Kerr measurements are carried out to study the precessional dynamics of ferromagnetic thin films with out-of-plane anisotropy. A combined analysis of parameters, such as coercive fields, magnetic anisotropy, and Gilbert damping α , is reported. Using a macrospin approximation and the Landau–Lifshitz–Gilbert equation, the effective anisotropy and α are obtained. A large damping varying with the applied field as well as with the thickness of the ferromagnetic layer is reported. Simulations using a distribution in the effective anisotropy allow us to reproduce the field evolution of α . Moreover, its thickness dependence correlates with the spin pumping effect. © 2009 American Institute of Physics. [DOI: 10.1063/1.3093816]

The magnetization dynamics of thin magnetic layers with perpendicular anisotropy is of great scientific and technological interest since they are potential candidates as high density magnetic media or in spintronics applications.^{1–3} Recent developments in the field of spin transfer torque in magnetic nanostructures emphasized the necessity to understand and control the physical processes involved in the magnetization dynamics. Indeed, the threshold current for magnetic excitation in nano-oscillators,^{4,5} the velocity of a magnetic domain wall, and the critical current required to trigger its motion⁶ as well as the timescale for magnetization reversal in future magnetic random access memories,⁷ depend on the magnetization relaxation and thus on the Gilbert damping α as can be described by the Landau–Lifshitz–Gilbert (LLG) equation of motion.^{8,9}

Magnetization dynamics of an ultrathin ferromagnetic (FM) layer sandwiched between two normal metal layers is also prone to interfacial effects such as the spin pumping effect.¹⁰ Namely, the spin current generated by a precessing magnetization can be absorbed by the normal metal in contact with the FM layer, thus increasing the effective damping of the system. In this letter, we used time resolved magneto-optical Kerr measurements to study the magnetization dynamics of a thin perpendicularly magnetized $\text{Co}_{48}\text{Fe}_{32}\text{B}_{20}$ (CoFeB in the following) layer. The use of an amorphous FM layer such as CoFeB is motivated by the desire to decrease the amount of pinning centers for domain wall motion applications. Altogether, the presented results give a full description of the magnetic properties of the system. Modifying certain parameters such as the magnetic anisotropy or the damping in a controlled way is the key to get a better insight into the physics of current induced domain wall motion in perpendicularly magnetized layers.

The samples used in this study consist of a Pt (4 nm)/CoFeB (t nm)/Pt (2 nm) trilayer grown at room temperature by dc magnetron sputtering onto a Si(001) substrate with a native oxide. Both Pt layers induce a strong interfacial perpendicular magnetic anisotropy pulling the CoFeB magnetization out of the film plane for a certain thickness range. The

magnetization dynamics was studied by polar time resolved magneto-optical Kerr effect (TRMOKE) measurements. A pulsed laser with a wavelength of 790 nm and a pulse width of 70 fs with a repetition rate of 80 MHz is used. The pump and the probe laser are focused down to the same $\sim 10 \mu\text{m}$ spot at almost perpendicular incidence. In this configuration, the measured Kerr rotation is proportional to the out-of-plane component of the magnetization. A variable magnetic field is applied at an angle of $\beta \approx 15^\circ$ from the plane resulting in a canting of the magnetization away from the out-of-plane anisotropy axis, as defined in Fig. 1(a). The angle β is restricted around $\approx 15^\circ$ due to space constraints. Figure 1(b) shows typical hysteresis loops for CoFeB layers with thickness varying from 0.45 to 0.65 nm with the magnetic applied field perpendicular to the film plane. In this range, the coercive field increases from 2 to 3 mT while the hysteresis loops are slightly slanted but with a 100% remanence, which is a first proof of the high out-of-plane anisotropy of our samples.

Figure 2(a) shows TRMOKE measurements obtained for a CoFeB thickness of 0.55 nm. The temporal scale is broken between 2 and 10 ps giving a clearer representation of the different temporal regimes occurring after excitation of the magnetization by a laser pulse.¹¹ During the first ~ 150 fs, the laser pulse creates a thermal excitation leading to a reduction in the magnetization of approximately 7% as well as a modification of the effective anisotropy. Then, a rather quick recovery of the magnetization is observed due to the balancing of electron and phonon energies with a time con-

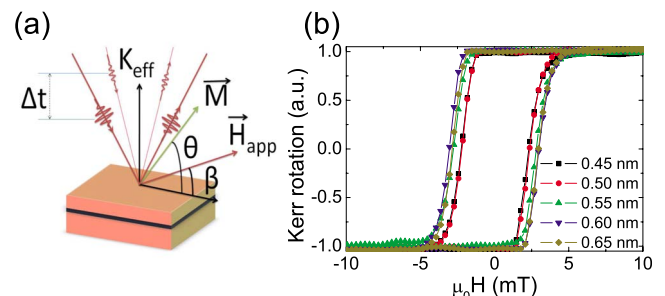


FIG. 1. (Color online) (a) Schematic of the TRMOKE setup. (b) Magnetic hysteresis loops for different CoFeB thicknesses.

^{a)}Electronic addresses: gregory.malinowski@gmail.com and g.malinowski@tue.nl.

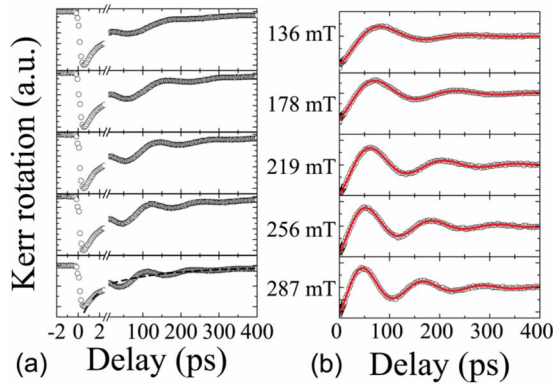


FIG. 2. (Color online) (a) Time resolved Kerr signal measured for different magnetic applied field and for a 0.55 nm CoFeB thick. The dashed line shows the double exponential background. (b) Same measurement after subtracting the background (see text). The red lines are fits to the data according to Eq. (1).

stant of ~ 500 fs, followed by a slower recovery of the magnetization due to heat diffusion into the sample. On a longer timescale after ~ 20 ps, a damped precession of the magnetization occurs following the change in the anisotropy induced during the laser excitation. After subtracting the demagnetization peak and the background shown as a dashed line in the bottom part of Fig. 2(a), oscillations in the Kerr rotation due to magnetization precession become more obvious [Fig. 2(b)]. The data can then be analyzed using an exponentially damped sine,

$$\Delta\theta_K \sim \sin(2\pi\nu t + \varphi) \exp\left(-\frac{t}{t_\alpha}\right), \quad (1)$$

where ν , t_α , and φ represent the oscillation frequency, the exponential decay time, and the phase, respectively. From a fit to the Kerr rotation spectra, we extracted the value of the frequency [Fig. 3(a), top]. For each thickness (not shown), a linear increase in the oscillation frequency is observed at high applied magnetic field. When the field is reduced a deviation from this linear behavior is seen which is mainly due to the geometrical configuration of our experimental setup [Fig. 1(a)]. Using a macrospin approximation and solving the LLG equation, the following analytical expression for the oscillation frequency is deduced,

$$\nu = \frac{\gamma\mu_0}{1 + \alpha^2} \left(H_{\text{app}} \frac{\sin(\beta)}{\sin(\theta)} + \frac{2K_{\text{eff}}}{\mu_0 M_S} - M_S \right), \quad (2)$$

where H_{app} , K_{eff} , and M_S are the applied magnetic field, the effective anisotropy, and the saturation magnetization, respectively. The nonlinearity in the evolution of the frequency with the applied field directly comes from the difference between the applied field direction represented by the angle β and the equilibrium direction of the magnetization represented by the angle θ . This appears in Eq. (2) as the ratio between the sine of those two angles. The angle θ corresponding to the equilibrium position of the magnetization is calculated by minimizing the energy of the system.

$$2\mu_0 H_{\text{app}} \sin(\theta - \beta) = \left(\frac{2K_{\text{eff}}}{M_S} - \mu_0 M_S \right) \sin(2\theta). \quad (3)$$

Using the last two equations and a saturation magnetization $M_S = 1200$ kA m $^{-1}$, the field evolution of the frequency was

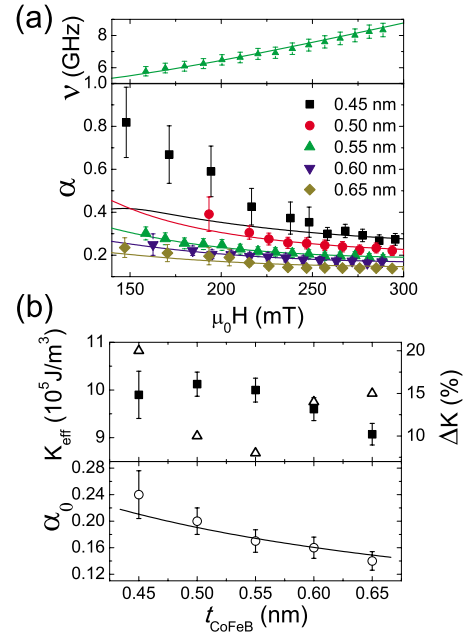


FIG. 3. (Color online) (a) Experimental and simulated static field dependence of the frequency (top) and of the Gilbert damping α (bottom) for various CoFeB thicknesses. (b) Evolution of the effective perpendicular anisotropy (square) and of the anisotropy distribution used in the simulation (triangle) for each CoFeB thickness (top). Variation in the high field limit of the damping α_0 (bottom) with the CoFeB thickness. The line corresponds to a fit in the data.

fitted and the effective perpendicular anisotropy extracted [Fig. 3(b), top]. Note that no change in M_S evaluated from superconducting quantum interference device measurements was noticed for reduced CoFeB thicknesses within a 10% error margin (not shown). The perpendicular effective anisotropy K_{eff} , first slightly increases with the thickness to reach a value of $\sim 1.0 \times 10^6$ J/m 3 before decreasing for thicker layers. For this CoFeB composition, the transition between out-of-plane and in-plane happens for a thickness of 0.75 nm. When deriving the Gilbert damping parameter, care has to be taken since the expression depends on the geometry of the experiment. In our configuration α is related to the damping time by

$$\alpha = (2\pi t_\alpha \nu)^{-1}, \quad (4)$$

in contrast to systems with in-plane magnetization, in which a more complicated expression is obtained.¹²

Based on Eq. (4), we estimated α and its field dependence is plotted in Fig. 3(a). For each CoFeB thickness, a similar evolution of α with the applied field is observed. In the high field regime α tends to be at a constant value, while it continuously increases when the field is reduced. Similar results have been reported recently in the case of a Py thin film and the increase in α was either ascribed to a distribution in the magnetic anisotropy¹² or to the excitation of multiple precessional modes.¹³ In the case of very thin films, the magnetization dynamics is known to be sensitive to local variation in the magnetic properties. Recently, Choe and Shin¹⁴ gave undeniable proofs that for Co based thin films, local variations in their magnetic properties display a distribution far from a Gaussian. Based on those results, we implemented a square distribution of the effective perpendicular anisotropy which modifies the effective field in the

LLG equation.^{15–17} The distribution is centered around the value of the anisotropy obtained from the fit of the oscillation frequency.

The calculated value of the oscillation frequency and the effective damping are plotted as full lines in Fig. 3(a). Regarding the effective Gilbert damping, a good agreement between the calculation and the measurements is generally obtained. A square distribution of the effective perpendicular anisotropy varying from 8.0% to 15.0% centered on K_{eff} [Fig. 3(b)] is used to simulate the large increase in the damping in the low field regime for a CoFeB thickness between 0.5 and 0.65 nm. The distribution seems to correlate with K_{eff} , the larger the effective anisotropy, the lower the distribution. In the case of 0.45 nm, it is not possible to reproduce the experimental data even with a distribution of 20%. For such a thin layer, the morphology of the film is not likely to be uniform resulting in dispersion in the thickness of the CoFeB layer. Hence, the high density of defects and inhomogeneities might increase the effective damping even further. Moreover, because of the high damping, too few oscillations are present in the Kerr rotation spectra to allow a good determination of the oscillation frequency and of the exponential decay time, resulting in a large error on the value of α .

From the simulated curve, we can extract the high field limit value of the damping α_0 . Those values are similar to the one reported in the case of Pt/Co/Pt multilayers.^{18,22} The variation in α_0 with the CoFeB thickness is plotted at the bottom of Fig. 3(b). A clear increase is observed when the CoFeB layer becomes thinner. The thickness dependence of α_0 might involve different mechanisms based on spin wave scattering and spin current dissipation. In the first case, inhomogeneities in a magnetic thin film such as defects or grain boundaries can strongly enhance the scattering of the uniform precessional mode into shorter wavelength spin waves. The density of defects is likely to increase when the film thickness is reduced. As a consequence, dissipation of the energy is faster resulting in a higher effective Gilbert damping. However, the influence of magnon scattering on the damping is less operative when the magnetization is perpendicular to the film plane.¹⁹ In the second case, the increase in α_0 for thinner CoFeB can be attributed to the spin pumping effect which is the most relevant mechanism in this very thin thickness range.^{10,20,21} The spin current generated by the precession of the magnetization which enters the Pt layers is completely absorbed because of the very low spin diffusion length of Pt. The dissipation of spin angular momentum in the Pt layer leads to an effective increase in the measured damping inversely proportional to the CoFeB thickness, as shown in Fig. 3(b). Hence, by only varying the CoFeB thickness, we can control the effective damping and therefore study its influence on current and field induced domain wall motion. However, a quantitative analysis of the spin pumping effect in those samples and its probable influence on the spin transfer effect would require a more detailed study.

In conclusion, we have studied the magnetization dynamics of perpendicularly magnetized Pt/CoFeB/Pt multilayers using time resolved magneto-optical Kerr effect measurements. From the damped precession of the magnetization, we obtained the effective perpendicular anisotropy and the Gilbert damping parameter. The large increase in α when the applied field is reduced can be explained by a distribution of the perpendicular anisotropy. Moreover, when the CoFeB layer thickness is reduced, an increase in the Gilbert damping is reported which is attributed to the spin pumping effect. Both the anisotropy distribution and the spin pumping effect, leading to a dissipation of the angular momentum, are crucial parameters to control the perspective of using perpendicularly magnetized layers in domain wall motion based applications. Finally, our approach provides a way to obtain information on the anisotropy distribution in patterned media of which knowledge is a prerequisite for their use as recording media.

- ¹D. Ravelosona, D. Lacour, J. A. Katine, B. D. Terris, and C. Chappert, *Phys. Rev. Lett.* **95**, 117203 (2005).
- ²S. Mangin, D. Ravelosona, J. A. Katine, M. J. Carrey, B. D. Terris, and E. Fullerton, *Nature Mater.* **5**, 210 (2006).
- ³O. Boulle, J. Kimling, P. Warnicke, M. Kläui, U. Rüdiger, G. Malinowski, H. J. M. Swagten, B. Koopmans, C. Ulysse, and G. Faini, *Phys. Rev. Lett.* **101**, 216601 (2008).
- ⁴D. Houssameddine, U. Ebels, B. Delaët, B. Rodmacq, I. Firastrau, F. Ponthenier, M. Brunet, C. Thirion, J.-P. Michel, L. Prejbeanu-Buda, M.-C. Cyrille, O. Redon, and B. Dieny, *Nature Mater.* **6**, 447 (2007).
- ⁵O. Boulle, V. Cros, J. Grollier, L. G. Pereira, C. Deranlot, F. Petroff, G. Faini, J. Barnas, and A. Fert, *Nat. Phys.* **3**, 492 (2007).
- ⁶L. Thomas and S. S. P. Parkin, *Handbook of Magnetism and Advanced Magnetic Materials 2* (Wiley, New York, 2007), pp. 942–982.
- ⁷T. Devolder, J. Hayakawa, K. Ito, H. Takahashi, S. Ikeda, P. Crozat, N. Zerounian, J.-V. Kim, C. Chappert, and H. Ohno, *Phys. Rev. Lett.* **100**, 057206 (2008).
- ⁸L. Landau and E. Lifshitz, *Phys. Z. Sowjetunion* **8**, 153 (1935).
- ⁹T. L. Gilbert, *Phys. Rev.* **100**, 1243 (1955).
- ¹⁰Y. Tserkovnyak, A. Brataas, and G. E. W. Bauer, *Phys. Rev. Lett.* **88**, 117601 (2002).
- ¹¹B. Koopmans, *Handbook of Magnetism and Advanced Magnetic Materials 3* (Wiley, New York, 2007), pp. 1589–1613.
- ¹²J. Walowski, M. Djordjevic Kaufmann, B. Lenk, C. Hamann, J. McCord, and M. Münzenberg, *J. Phys. D* **41**, 164016 (2008).
- ¹³S. Serrano-Guisan, K. Rott, G. Reiss, and H. W. Schumacher, *J. Phys. D* **41**, 164015 (2008).
- ¹⁴S.-B. Choe and S. Sung-chul, *Phys. Rev. B* **65**, 224424 (2002).
- ¹⁵B. Heinrich, J. F. Cochran, and R. Hasegawa, *J. Appl. Phys.* **57**, 3690 (1985).
- ¹⁶Z. Celinski and B. Heinrich, *J. Appl. Phys.* **70**, 5935 (1991).
- ¹⁷R. D. McMichael, *J. Appl. Phys.* **103**, 07B114 (2008).
- ¹⁸A. Barman, S. Wang, O. Hellwig, A. Berger, E. E. Fullerton, and H. Schmidt, *J. Appl. Phys.* **101**, 09D102 (2007).
- ¹⁹R. Arias and D. L. Mills, *Phys. Rev. B* **60**, 7395 (1999); P. Landeros, R. E. Arias, and D. L. Mills, *ibid.* **77**, 214405 (2008).
- ²⁰M. V. Costache, M. Sladkov, S. M. Watts, C. H. van der Wal, and B. J. van Wees, *Phys. Rev. Lett.* **97**, 216603 (2006).
- ²¹J.-M. L. Beaujour, J. H. Lee, A. D. Kent, K. Krycka, and C.-C. Kao, *Phys. Rev. B* **74**, 214405 (2006).
- ²²P. J. Metaxas, J. P. Jamet, A. Mougin, M. Cormier, J. Ferré, V. Baltz, B. Rodmacq, B. Dieny, and R. L. Stamps, *Phys. Rev. Lett.* **99**, 217208 (2007).